Neuron, Volume *75*

Supplemental Information

Striatal Dopamine Release Is Triggered by Synchronized Activity in Cholinergic Interneurons

Sarah Threlfell, Tatjana Lalic, Nicola J. Platt, Katie A. Jennings, Karl Deisseroth, and Stephanie J. Cragg

Fig S1

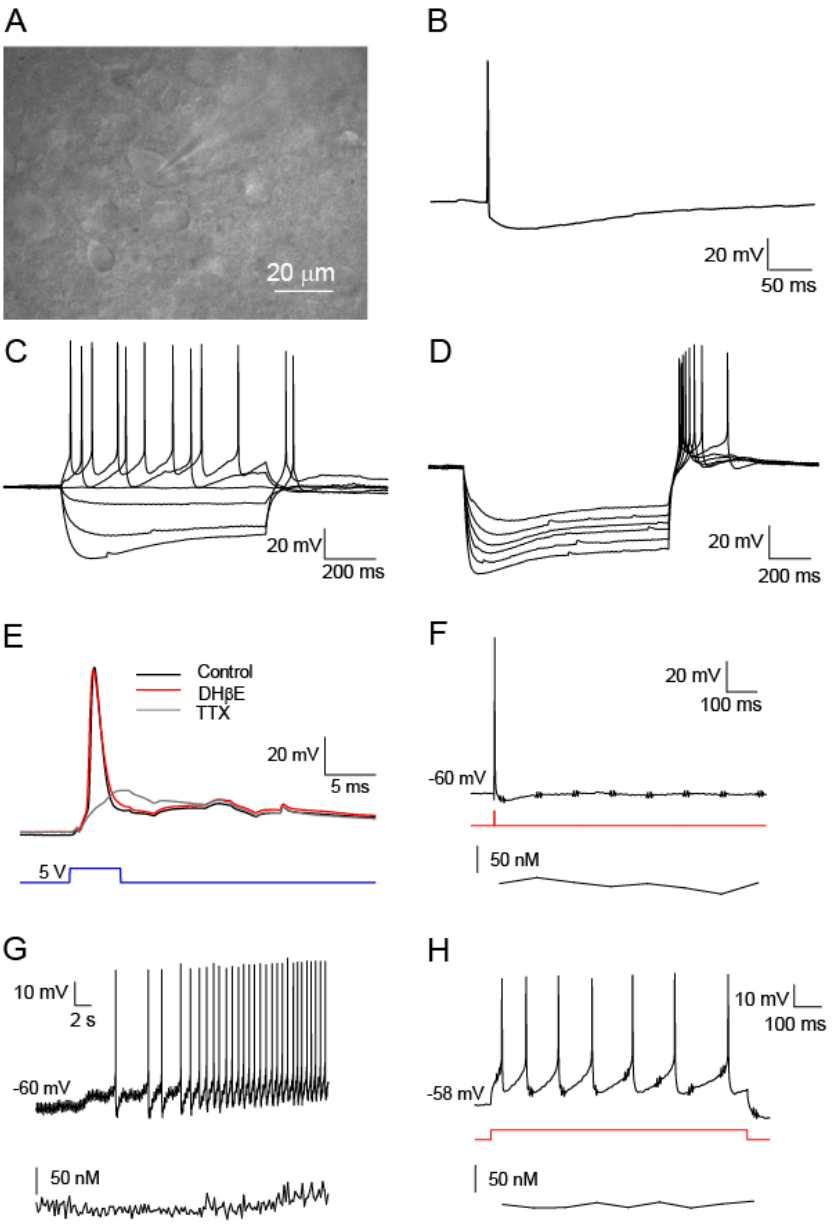

Figure S1, related to Figure 2. Manipulation of activity in individual ChIs is not sufficient to evoke DA release. (**A**) IR-DIC image of acute striatal slice containing ChI. (**B**) Whole cell current clamp recordings of single AP evoked by current injection. Note large amplitude and long lasting AHP, a hallmark feature of striatal ChIs. (**C**) Regular spiking evoked by depolarising current step. (**D**) Hyperpolarizing pulses induce a sag in the membrane potential response which depends on Ih activation. (**E**) Light-evoked AP waveform is unaffected by DHβE (1 μM) but abolished by TTX (1 μM). (**F-H)** Upper traces, ChI activity; Middle red (F,H only), current injection (1 nA); Lower, time-locked DA signal at CFM. Electrode configurations (patch electrode and CFM) as per laser-evoked recordings in **Fig. 2**. (**F**) Single AP evoked by current injection (2 ms) is not sufficient to evoke DA release. (**G**) Gradual increase in holding current induces tonic firing in ChI but no detectable DA release. (**H**) Longer duration current step (1 sec) induces AP burst and no DA release.

Fig S2

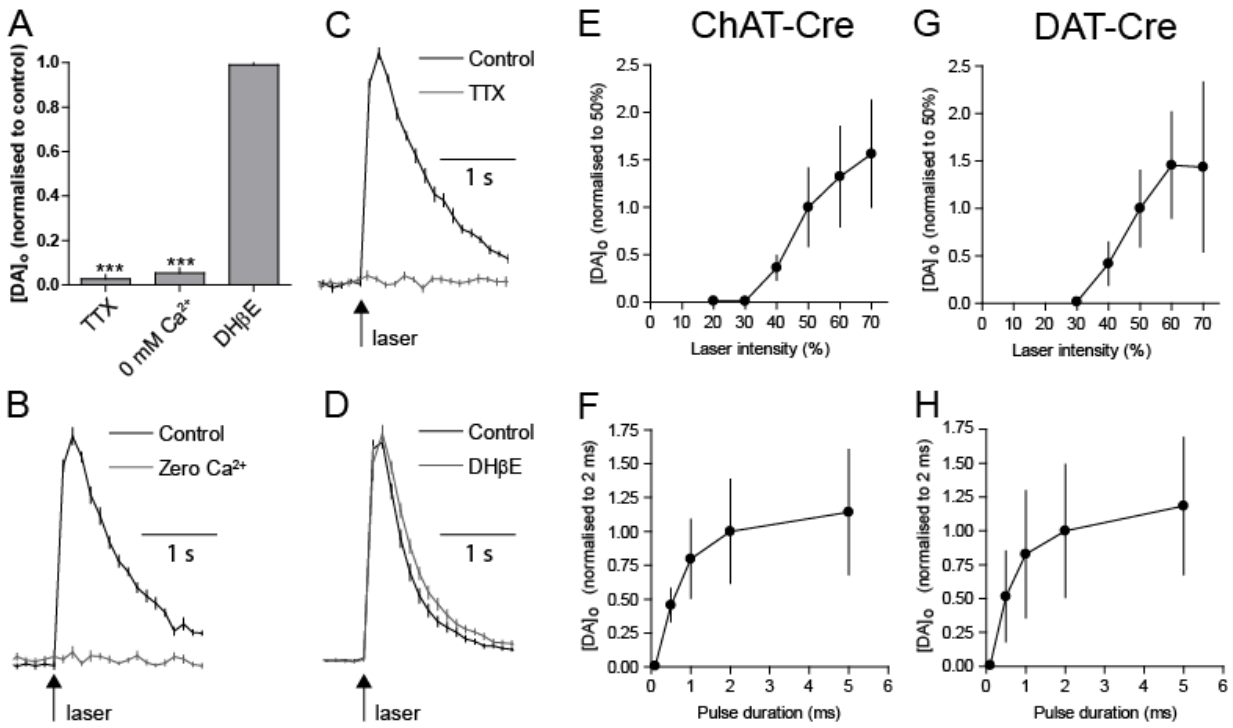

Figure S2, related to Figure 3. Pharmacological properties and laser-power and pulse-duration responsiveness of DA release in striatal slices from ChAT-Cre or DAT-Cre mice expressing ChR2 in ChIs or DA axons. (**A**) Single laser pulse evoked DA release in striatal slices expressing ChR2-eYFP in DA axons was abolished following removal of Ca^{2+} from recording aCSF, blockade of Na_v^+-channels with TTX (1 µM; n = 6-9, P<0.001), but in contrast to ChI-driven DA release, unaltered following blockade of nAChRs with DHβE(1 µM). (**B,C,D**) Profiles of mean $[DA]_o$ ± SEM versus time in CPu after single laser pulse stimuli in control versus drug conditions n = 6-11. Light-evoked DA release in striatal slices from DAT-Cre mice is independent of nAChRs, (n =11, P>0.05). (**E-H**) Relationship of laser-evoked DA release to (E,G) laser power and (F,H) pulse duration in striatal slices from (E,F) ChAT-Cre or (G,H) DAT-Cre mice. (**E,G**) Mean peak light-evoked extracellular DA ($[DA]_o$) increases with increasing laser power (pulse duration fixed at 2 ms). (**F,H**) Mean peak light-evoked $[DA]_o$ increases with increasing pulse duration (laser power fixed at 50%/10 mW/mm^2). Laser-evoked data in main figure used peri-maximal powers and durations (50-60%/10-40 mW/mm^2 and 1-2 ms), unless otherwise specified.

Table S1

	Laser intensity or current	V_m (mV)	Action potential half-width (ms)	Latency to spike (ms)	R_{INPUT} (MΩ)
ChAT-cre laser (n=11)	50 %	-57.2 ± 0.6	1.0 ± 0.1	2.0 ± 0.5	218.9± 22.9
ChAT-cre current (n=11)	1 nA	-58.9 ± 0.8	0.8 ± 0.1	-	
C57BL/6 current (n=8)	1 nA	-57.1 ± 2.0	0.9 ± 0.1	-	256.3 ± 36.5

Table S1, related to Figure S1. Summary of the basic electrophysiological properties of recorded ChIs. V_m, Resting membrane potential, R_{INPUT} input resistance, n = number of cells and animals.

SUPPLEMENTAL EXPERIMENTAL PROCEDURES

Animals and virus injections

Mice were group-housed on a 12 hr light/dark cycle and provided with food and water ad libitum. All procedures involving animals were performed according to methods approved by the United Kingdom Home Office and The Animals (Scientific Procedures) Act, 1986.

To generate expression of ChR2 in ChIs, DA neurons, or thalamostriatal glutamate inputs, we used a Cre-loxP approach by injecting a Cre-inducible recombinant AAV vector containing ChR2 (pAAV-double floxed-hChR2(H134R)-EYFP-WPRE-pA), in mice expressing Cre-recombinase in either choline acetyltransferase (ChAT)-, dopamine transporter (DAT)-, or Ca^{2+}-calmodulin dependent kinase II (CaMKII)-positive neurons respectively. Transgenic mice were bred from homozygotes for ChAT-internal ribosome entry site (IRES)-Cre, DAT-IRES-Cre, or CaMKII-Cre obtained from Jackson laboratories (B6.129S6-*Chat*$^{tm1(cre)Lowl}$/J, stock # 006410; B6.SJL-*Slc6a3*$^{tm1.1(cre)Bkmn}$ /J, stock # 006660; B6.Cg-Tg(Camk2a-cre)T29-1Stl/J, stock # 005359). The experimental data presented in this paper are from ChAT-Cre homozygote (and heterozygote, not illustrated), DAT-Cre heterozygote or CaMKII-Cre homozygote mice aged 2-8 months. Mice were anaesthetised with isoflurane, placed in a stereotaxic frame and a craniotomy was performed. Bilateral intracerebral injections of a Cre-inducible recombinant AAV (1 µl per site for ChAT and DAT mice, 300 nl per site for CaMKII-cre mice) were made with a 2.5 µl, 33 gauge Hamilton syringe using a microinjector at 0.2 µl/min. In ChAT-Cre mice, injections were made in dorsal CPu (AP +1.0 mm, ML ±1.8 mm, DV -2.2 mm) and in contralateral NAc core (AP +1.0 mm, ML ±1.0 mm, DV -4.0 mm). In DAT-Cre mice, injections were made in SNc (AP -3.5 mm, ML ±1.2 mm, DV -4.0 mm) and in contralateral VTA (AP -3.1 mm, ML ±0.5 mm, DV -4.4 mm). In CaMKII-Cre mice, injections were made in the intralaminar nucleus of the thalamus (AP -2.3, ML ± 0.5, DV -3.4 mm). Wildtype C57BL/6 mice used in some experiments were aged P14-P22.

Virus production and typing

To generate cell-specific expression of ChR2, we used a Cre-loxP approach; combining a Cre-inducible recombinant AAV vector (pAAV-double floxed-hChR2(H134R)-EYFP-WPRE-pA), with mice expressing Cre-recombinase in desired cell populations (i.e. DAT-Cre, ChAT-Cre and CaMKII-Cre obtained from Jackson laboratories) as described previously (Witten et al., 2010; Zhang et al., 2010). Cre-inducible recombinant AAV vectors were serotyped with AAV5 coat proteins and packaged by the viral vector core at the University of North Carolina to a final viral concentration of 1×10^{12} particles/ml.

Slice preparation

On days 12-76 post-injection, mice were decapitated after cervical dislocation or halothane anaesthesia (for combined patch-clamp/FCV recordings). A minimum of 12 days were allowed

post-injection to allow sufficient time for expression of ChR2 as suggested in literature (Yizhar et al., 2011; Zhang et al., 2010). Coronal slices, 300 µm-thick containing CPu and NAc were prepared as specified below for FCV and/or electrophysiology in ice-cold HEPES-buffered aCSF or high sucrose aCSF saturated with 95% O_2/5% CO_2. Slices were then maintained in a bicarbonate-buffered aCSF at room temperature prior to recording. During recordings, neurons were visualised on an upright microscope (Olympus BX51WI) equipped with IR-DIC, fluorescence optics for visualising eYFP and a charge-coupled device (CCD) camera.

A deficit in expression of endogenous DAT occurs in DAT-Cre mice irrespective of injections, and is less pronounced in heterozygotes than in homozygotes (Backman et al., 2006). We confirmed that DA uptake is only marginally modified in DAT-Cre heterozygous mice from analysis of DA clearance curves after evoked DA release. This modification is not responsible for the properties of DA release described here (data not illustrated).

Fast-scan cyclic voltammetry (FCV)

FCV experiments used an ice-cold HEPES-based buffer for slicing containing (in mM) NaCl (120), KCl (5), $NaHCO_3$ (20), HEPES acid (6.7), HEPES salt (3.3), $CaCl_2$ (2), $MgSO_4$ (2), KH_2PO_4 (1.2) and glucose (10), saturated with 95% O_2/5% CO_2. A bicarbonate-buffered artificial cerebrospinal fluid (aCSF) maintained at 30-32 °C was used for recording as described previously (Rice and Cragg, 2004; Threlfell et al., 2010) and contained (in mM): NaCl (124), KCl (3.7), $NaHCO_3$ (26), $CaCl_2$ (2.4), $MgSO_4$ (1.3), KH_2PO_4 (1.3), and glucose (10) saturated with 95% O_2/5% CO_2. Superfusion flow rate was approx 1.5-2 ml/min. Extracellular DA concentration ($[DA]_o$) was monitored using fast-scan cyclic voltammetry (FCV) with 7 µm diameter carbon fiber microelectrodes (CFMs; tip length 50–100 µm) and a Millar voltammeter (Julian Millar, Barts and the London School of Medicine and Dentistry, London, UK) as described previously (Threlfell et al., 2010). In brief, the scanning voltage was a triangular waveform (−0.7 to +1.3 V range vs. Ag/AgCl) at a scan rate of 800 V/s and sampling frequency of 8 Hz. Electrodes were calibrated in 1-2 µM DA in each experimental media.

Data were digitized at 50 kHz using Digidata 1440A acquisition board and analysed off-line using Axoscope 10.3 and locally written programs. Evoked currents were attributed to DA by comparison of the potentials for peak oxidation and reduction currents with those of DA in calibration media (+500–600 and −200 mV vs Ag/AgCl, respectively). Currents sampled at the DA oxidation peak potential to provide profiles of $[DA]_o$ versus time were measured in each voltammogram from baselines on which the oxidation current was superimposed. This procedure minimizes inclusion of contributions from other electroactive and non-electroactive species to the neurotransmitter oxidation current (Venton et al., 2003). Calibration solutions were made immediately before use from stock solutions of DA stored in 0.1 M $HClO_4$. Electrode sensitivity to DA was between 10 and 30 nA/µM.

Electrophysiology

For whole-cell patch clamp studies (in isolation or in combination with FCV), 300 µm coronal slices containing CPu and NAc were prepared in ice-cold high sucrose aCSF containing (in mM): NaCl (85), $NaHCO_3$ (25), 2KCl (2.5), NaH_2PO_4 (1.25), 0.5 $CaCl_2$, $MgCl_2$ (7), glucose (10), sucrose (75), following decapitation under halothane anaesthesia. Slices were then transferred to oxygenated aCSF (95% O_2, 5% CO_2) containing (in mM): NaCl (130), $NaHCO_3$ (25), KCl (2.5), NaH_2PO_4 (1.25), $CaCl_2$ (2), $MgCl_2$ (2), glucose (10) at 35°C for 30-45 minutes and then maintained at room temperature until recording. During recordings, slices were superfused with aCSF saturated with 95% O_2/5% CO_2 at 32 ºC. Whole cell patch clamp electrodes (4-7 MΩ) were filled with an intracellular solution containing (in mM): K-gluconate (120), KCl (10), HEPES (10), MgATP (4), NaGTP (0.3), Na-phosphocreatine (10) and 0.5% biocytin. ChIs in the striatum were identified by their distinctive morphological features (**Figure S1A**) (large somas and thick primary dendrites) and their characteristic electrophysiological properties: prominent Ih, AHP and broad action potential (**Figures S1B-S1D, Table S1**). Intracellular recordings were obtained using a Multiclamp 700B amplifier and digitized at 10-20 kHz using Digidata 1440A acquisition board. While performing current clamp recordings, a small amount of holding current (typically < -25 pA) was injected when necessary to keep the cell close to its initial resting membrane potential (-60 mV). Biocytin was included in the intracellular solution to allow post-hoc visualization and confirmation of cell identity. All data were analysed offline with Clampfit (pClamp 10), Neuromatic http://neuromatic.thinkrandom.com) and custom-written software running within IgorPro environment.

Combined electrophysiology and FCV recordings

The carbon fibre microelectrode used for FCV recordings was placed into striatal tissue and charged by scanning the voltammeter whilst the slice equilibrated in the recording chamber (20 -30 mins). The voltammeter was then turned off, and an eYFP+ve ChI was patched in close proximity to the CFM (200-320 µm). Basic electrophysiological features were monitored thoughout the experiment (eg: input resistance, spike threshold, Ih etc). We were able to simultaneously acquire both the whole-cell membrane potential and DA release, during current-evoked and light-evoked ChI activity paradigms, without any perturbations of the cell properties with exception of small artefact (~5 mV) induced by the scanning voltage waveform every 125 ms. Laser stimulation did not alter the properties of the cell (data not shown).

Light and electrical stimulation

ChR2-expressing fibres were activated using a 473 nm diode laser (DL-473, Rapp Optoelectronic) coupled to the microscope with a fiber optic cable (200 µm multimode, NA 0.22) which illuminated a 15-60 µm diameter spot (40 x/10 x water-immersion objectives) or, in CaMKII experiments, an LED system (OptoLED, CAIRN). TTL-driven laser pulses (1-2 ms duration, 2-40 mW/mm^2 at specimen) or electrical pulses (0.6-0.7 mA, 200 µs) were delivered at

a variety of frequencies designed to mimic physiological firing frequencies. Light power at microscope objective exit was 2-40 mW/mm^2 (see **Figure S2**). For experiments assessing responsiveness to increasing pulse duration and laser power using slices from ChAT-Cre or DAT-Cre mice, TTL pulse duration was varied between 100 µs and 5 ms, and laser intensity was varied between 20 and 70% (0 – 90 mW/mm^2 at objective exit; see **Figure S2**).

For experiments assessing effects of driving thalamostriatal input in striatal slices from CaMKII-Cre mice, an LED system (OptoLED, CAIRN) was used to activate ChR2-expressing fibres. This LED system was coupled directly to the microscope via the fluorescence arm, and provides full-field illumination of the brain slice, activating all ChR2-expressing fibres in the field of view. TTL-driven light pulses (2 ms duration, 8.0 current) were delivered at a variety of frequencies designed to mimic physiological firing frequencies. Trains of pulses (4, 25 or 50 pulses at 25 Hz) did not evoke significantly more DA release than that following single pulse stimulation in striatal slices from CaMKII-Cre mice. Once a release site was located we used single pulse activation every 2.5 minutes, prior to pharmacological investigations.

Electrical stimulation was delivered by a local bipolar concentric electrode (25 µm-diameter, Pt/Ir; FHC, USA). Both light and electrical stimuli were delivered locally; the laser spot was out of field of view of the CFM (~200-300 µm from CFM) and stimulating electrode was placed ~150 µm from the CFM. Mean peak light-evoked $[DA]_o$ in dorsal CPu from ChAT-Cre (1.4 ± 0.2 µM) or DAT-Cre (1.0 ± 0.1 µM) was not significantly different (n = 24, P>0.05). Data presented here is from dorsal CPu; however we made similar observations in NAc (data not shown). Mean peak light-evoked $[DA]_o$ in dorsal CPu from CaMKII-Cre mice with ChR2-expressing thalamostriatal inputs was 0.42 ± 0.05 µM (n=59).

Immunocytochemistry

To determine the specificity of ChR2 expression in ChAT-Cre or DAT-Cre mice, acute striatal (ChAT) or midbrain slices (DAT) containing ChR2-eYFP positive neurons were fixed at the end of recordings in 4% paraformaldehyde dissolved in phosphate-buffered saline (PBS) containing 0.2% picric acid. Slices were fixed overnight at 4°C and then stored in PBS until re-sectioning to 40 µm. Free-floating sections were then washed in PBS and incubated in 0.5% Triton X-100 and 10% normal donkey serum (ChAT) or 10% goat and fetal bovine serum (DAT). Slices were subsequently incubated with primary antibody dissolved in PBS containing 0.5% Triton X-100 and 3% normal donkey serum (goat anti-ChAT 1:200; Millipore) or PBS containing 0.5% Triton X-100 and 1% normal goat and fetal bovine serum (rabbit anti-TH 1:2000; Sigma) at 4°C overnight. Sections were then washed with PBS and incubated for 2 hours at room temperature with secondary antibody dissolved in PBS containing 0.5% Triton X-100 and 3% normal donkey serum (1:1000 Alexa Fluor 568 donkey anti-goat, Invitrogen) or PBS containing 0.5% Triton X-100 and 1% normal goat and fetal bovine serum (1:1000 DyLight 594 goat anti-rabbit, Jackson). In order to verify the identity of recorded neurons, Alexa 488-conjugated streptavidin (Invitrogen)

was included in the secondary antibody solution at a final concentration of 1:250. Slices were then washed with PBS and mounted on gelled slides with Vectashield mounting medium (Vector Labs) and imaged using an AxioSkop fluorescent microscope (Zeiss).

Statistical Analysis

Data are represented as means ± SEM, '*n*' refers to the number of observations. The number of animals in each data set is ≥ 3. Data for DA are expressed as extracellular concentration of dopamine ($[DA]_o$), or as $[DA]_o$ normalized to a single pulse in control. Comparisons for statistical significance were assessed by one- or two-way ANOVA and post hoc multiple-comparison t-tests, or unpaired t-tests using GraphPad Prism. Levels of DA indicated either following current-induced activity in ChIs (**Figures S1F-S1H**) or while gradually increasing laser power from 0 mW/mm^2 until spike threshold is reached in single ChIs (**Figure 2C**), were indistinguishable from noise.

Drugs

D(-)-2-Amino-5-phosphonovaleric acid (D-AP5), 4-(8-methyl-9*H*-1,3-dioxolo[4,5-*h*][2,3]benzo-diazepin-5-yl)-benzenamine hydrochloride (GYKI 52466 hydrochloride), (*S*)-α-methyl-4-carboxy-phenylglycine [(*S*)-MCPG], oxotremorine-M (Oxo-M), bicuculline methiodide and saclofen were purchased from Tocris Bioscience or Ascent Scientific. Atropine, dihydro-β-erythroidine (DHβE) and all other reagents were purchased from Sigma-Aldrich. Drugs were dissolved in distilled water, aqueous alkali [(*S*)-MCPG] or aqueous acid (GYKI 52466 hydrochloride) to make stock aliquots at 1000–10000 × final concentrations, and stored at −20°C until required. Stock aliquots were diluted with oxygenated aCSF to final concentration immediately before use.

SUPPLEMENTAL REFERENCES

Backman, C.M., Malik, N., Zhang, Y., Shan, L., Grinberg, A., Hoffer, B.J., Westphal, H., and Tomac, A.C. (2006). Characterization of a mouse strain expressing Cre recombinase from the 3' untranslated region of the dopamine transporter locus. Genesis *44*, 383-390.

Rice, M.E., and Cragg, S.J. (2004). Nicotine amplifies reward-related dopamine signals in striatum. Nat Neurosci *7*, 583-584.

Threlfell, S., Clements, M.A., Khodai, T., Pienaar, I.S., Exley, R., Wess, J., and Cragg, S.J. (2010). Striatal muscarinic receptors promote activity dependence of dopamine transmission via distinct receptor subtypes on cholinergic interneurons in ventral versus dorsal striatum. J Neurosci 30, 3398-3408.

Venton, B.J., Michael, D.J., and Wightman, R.M. (2003). Correlation of local changes in extracellular oxygen and pH that accompany dopaminergic terminal activity in the rat caudate-putamen. J Neurochem *84*, 373-381.

Witten, I.B., Lin, S.C., Brodsky, M., Prakash, R., Diester, I., Anikeeva, P., Gradinaru, V., Ramakrishnan, C., and Deisseroth, K. (2010). Cholinergic interneurons control local circuit activity and cocaine conditioning. Science *330*, 1677-1681.

Yizhar, O., Fenno, L.E., Davidson, T.J., Mogri, M., and Deisseroth, K. (2011). Optogenetics in neural systems. Neuron *71*, 9-34.

Zhang, F., Gradinaru, V., Adamantidis, A.R., Durand, R., Airan, R.D., de Lecea, L., and Deisseroth, K. (2010). Optogenetic interrogation of neural circuits: technology for probing mammalian brain structures. Nat Protoc *5*, 439-456.